ORIGINAL RESEARCH

Development of Aortic Valve Disease in Familial Hypercholesterolemic Swine: Implications for Elucidating Disease Etiology

Ana M. Porras, MS; Dhanansayan Shanmuganayagam, PhD; Jennifer J. Meudt, MS; Christian G. Krueger, BS; Timothy A. Hacker, PhD; Peter S. Rahko, MD; Jess D. Reed, PhD; Kristyn S. Masters, PhD

***Background*—**Familial hypercholesterolemia (FH) is a prevalent hereditary disease associated with increased atherosclerosis and calcific aortic valve disease (CAVD). However, in both FH and non-FH individuals, the role of hypercholesterolemia in the development of CAVD is poorly understood. This study used Rapacz FH (RFH) swine, an established model of human FH, to investigate the role of hypercholesterolemia alone in the initiation and progression of CAVD. The valves of RFH swine have not previously been examined.

***Methods and Results*—**Aortic valve leaflets were isolated from wild-type (0.25- and 1-year-old) and RFH (0.25-, 1-, 2-, and 3-year-old) swine. Adult RFH animals exhibited numerous hallmarks of early CAVD. Significant leaflet thickening was found in adult RFH swine, accompanied by extensive extracellular matrix remodeling, including proteoglycan enrichment, collagen disorganization, and elastin fragmentation. Increased lipid oxidation and infiltration of macrophages were also evident in adult RFH swine. Intracardiac echocardiography revealed mild aortic valve sclerosis in some of the adult RFH animals, but unimpaired valve function. Microarray analysis of valves from adult versus juvenile RFH animals revealed significant upregulation of inflammation-related genes, as well as several commonalities with atherosclerosis and overlap with human CAVD.

***Conclusions*—**Adult RFH swine exhibited several hallmarks of early human CAVD, suggesting potential for these animals to help elucidate CAVD etiology in both FH and non-FH individuals. The development of advanced atherosclerotic lesions, but only early-stage CAVD, in RFH swine supports the hypothesis of an initial shared disease process, with additional stimulation necessary for further progression of CAVD. **(*J Am Heart Assoc*. 2015;4:e002254 doi: 10.1161/JAHA.115.002254)**

Key Words: aortic valve • cardiovascular diseases • hypercholesterolemia

Familial hypercholesterolemia (FH) is one of the most common hereditary diseases in the Western Hemisphere, affecting 1 in every 244 individuals.[1] FH is a disorder of lipoprotein metabolism often caused by mutations in the low-density lipoprotein (LDL) receptor, leading to high circulating levels of LDL.[2–4] Numerous studies have established a relationship between FH and a high risk of atherosclerosis at a young age.[5–7]

From the Division of Cardiovascular Medicine, Departments of Medicine (T.A.H., P.S.R.), Biomedical Engineering (A.M.P., K.S.M.), and Animal Sciences (D.S., J.J.M., C.G.K., J.D.R.), University of Wisconsin–Madison, Madison, WI.

Accompanying Data S1, Figures S1 through S5, Tables S1 and S2, and Videos S1 and S2 are available at http://jaha.ahajournals.org/content/4/10/e002254/suppl/DC1

Correspondence to: Kristyn S. Masters, PhD, Department of Biomedical Engineering, University of Wisconsin-Madison, 1550 Engineering Dr, #2152, Madison, WI 53706. E-mail: kmasters@wisc.edu

Received May 28, 2015; accepted September 22, 2015.

A somewhat lesser appreciated impact of FH is the increased risk of developing calcific aortic valve disease (CAVD). Although less studied than atherosclerosis in FH, the increased incidence of CAVD in FH patients is significant, with over half of homozygous FH (HoFH) males and 21% to 41% of HoFH females exhibiting aortic regurgitation or more-advanced valvular dysfunction.[8,9] This correlation is not entirely unexpected, given that CAVD has been associated with hyperlipidemia,[10] and stenotic valves are rich in oxidized lipids and apolipoproteins B and E.[11,12] However, in contrast to coronary artery disease (CAD), elevated LDL is considered a relatively weak risk factor for CAVD.[10,13]

Much remains to be learned about the relationship between hypercholesterolemia and CAVD, both within the FH population and more broadly. The many conflicting reports on the use of statins (3-hydroxy-3-methylglutaryl-coenzyme A reductase inhibitors) to prevent or treat CAVD serve to illustrate this point.[14–16] Although these LDL-lowering drugs are considered an effective therapy for reducing the incidence or severity of CAD in both FH[17,18] and non-FH populations,[19,20] randomized, prospective trials have failed to yield evidence that statins are effective at reducing the progression

of CAVD.[21–23] Even in individuals with FH, it remains unclear to what extent elevated LDL levels may contribute to initiation or progression of aortic valve disease. Developing an improved understanding of the role that elevated LDL plays in the onset and progression of CAVD can help to better refine potential treatment options for both FH and non-FH individuals.

Characterization of aortic valves from Rapacz familial hypercholesterolemic (RFH) swine offers the opportunity to examine the relationship between FH and onset of valvular pathology, independent of other risk factors. RFH swine express elevated LDL levels as a result of a mutation in the gene encoding the LDL receptor (LDL-R),[24] as is commonly observed in humans with FH. Due to their ability to develop complex atherosclerotic lesions that closely mimic those found in humans, these animals have been used extensively in the study of atherosclerosis over the past 2 decades,[25] as well as in the development and validation of therapeutic and diagnostic cardiovascular technologies.[26,27] However, the heart valves of RFH swine have not previously been evaluated. This study examines the aortic valves of adult RFH swine to investigate the relationship between FH and CAVD, as well as determine whether RFH swine may serve as an animal model for CAVD.

Materials and Methods

All reagents were obtained from Sigma-Aldrich (St Louis, MO), unless noted otherwise. An expanded methods section is available in Data S1.

Experimental Animal Model

This study conformed to the National Institutes of Health (NIH) guidelines on the care and use of laboratory animals, as well as the guidelines of the University of Wisconsin–Madison Institutional Animal Care and Use Committee. A total of 21 female animals were included: 4 juvenile (0.25-year-old) wild-type (WT) swine, 3 one-year-old (1 yo) WT swine, 3 juvenile (0.25 yo) RFH swine, 4 two-year-old (2 yo) adult RFH swine, and 5 three-year-old (3 yo) RFH swine (Table 1), with all RFH swine possessing a homozygous mutation. The WT swine used in this study are from a genetic line that was derived from the RFH line to be absent of LDL-R mutation; thus, the WT swine have normal cholesterol levels and do not develop atherosclerosis on a standard diet. The animals were maintained on a standard swine diet (75.8%, 14.7%, and 9.4% of daily calories from carbohydrates, protein, and fat, respectively) throughout the duration of the study. The animals were stunned and euthanized by exsanguination for tissue collection. After euthanasia, the heart was excised and rinsed in saline. The left ascending, left circumflex, and right coronary arteries were carefully dissected and fixed in 10% formalin. Likewise, leaflets were dissected from the aortic valves and immediately fixed in 10% formalin or placed in RNAlater.

Serum Cholesterol Level Measurements

Whole blood was collected during exsanguination and allowed to clot in serum collection tubes. Collection tubes were centrifuged at 1200*g* for 7 minutes; serum was stored at 4°C and analyzed for cholesterol within 24 hours of collection. Serum cholesterol levels were measured on a Vitros 5,1 FS Chemistry System (Ortho-Clinical Diagnostics, Inc, Rochester, NY) using multilayer film dry-slide chemistry with colorimetric detection according to manufacturer's recommendations. Porcine cholesterol values were converted to equivalent human cholesterol values according to the findings of Swinkels et al.[28]

Intracardiac Echocardiography

The five 3-yo RFH swine were anesthetized with a combination of telazol (a solution of 50 mg/mL of tiletamine and 50 mg/mL of zolazepam administered at 1 to 8 mg/kg, intramuscularly) and xylazine (0.2 to 2.2 mg/kg, intramuscularly) and intubated. General anesthesia was maintained with 1.5% to 3.5% isoflurane delivered in 100% oxygen at a flow rate of 1 to

Table 1. Serum Cholesterol Levels of WT and RFH Swine

Variable	WT Juvenile	WT 1 yo	RFH Juvenile	RFH 1 yo	RFH 2 yo	RFH 3 yo
Number of animals	4	3	3	3	4	5
Age, y	0.29 (0.02)	0.92 (0.01)	0.23 (0.01)	0.92 (0.01)	2.5 (0.05)	3.4 (0.15)
Weight, kg	8.70 (1.20)	63.5 (13.5)	9.30 (1.30)	54.0 (9.60)	151 (25.6)	111 (5.20)
Cholesterol, mg/dL	119 (12.4)	121 (25.7)	341 (59.0)	495 (97.5)	408 (20.6)	273 (70.2)
Equivalent human cholesterol, mg/dL[28]	238 (24.8)	243 (51.4)	609 (118)	990 (195)	817 (41.2)	545 (140)

RFH indicates Rapacz familial hypercholesterolemic; WT, wild-type.

3 L/min by a ventilator. A Siemens AcuNav 8F ultrasound catheter (Siemens, Mountain View, CA) was introduced and guided into the right ventricle by a vascular sheath percutaneously placed in the femoral vein. Ultrasound images of the aortic valve were captured using an Acuson Cypress Plus Ultrasound imaging system (Siemens) and are presented as cross-sectional views of the valve. Heart valve function was also assessed by the color Doppler imaging mode. After the intracardiac echocardiography (ICE) procedure, animals were recovered and maintained on standard husbandry until subsequent postmortem tissue collection several months later.

Histological Characterization

Formalin-fixed leaflets and coronary arteries were embedded in paraffin and cut into 6-μm-thick sections. Sections were stained with hematoxylin and eosin (H&E) or Movat's pentachrome (Poly Scientific, Bay Shore, NY). After histological staining, leaflet thickness was measured using ImageJ software (NIH, Bethesda, MD). Tissue sections were deparaffinized and antigen retrieval was performed in citric acid buffer (pH 6.0; Vector Laboratories, Burlingame, CA) for 2 hours in a water bath at 80°C. Detection of cleaved caspase 3 (2 μg/mL, polyclonal, rabbit; Cell Signaling Technology, Inc., Danvers, MA), CD107a (5 μg/mL, polyclonal, mouse; AbdSerotec, Raleigh, NC), monocyte chemoattractant protein 1 (MCP-1; 5 μg/mL, polyclonal, rabbit; PeproTech, Rocky Hill, NJ), oxidatively modified apolipoprotein-B100 (oxApoB; 10 μg/mL, polyclonal, mouse), and malondialdehyde (MDA; 10 μg/mL, polyclonal, mouse) was performed using immunohistochemical methods following the VECTASTAIN Universal Elite ABC Kit protocol (Vector Laboratories). Alpha-smooth muscle actin (αSMA, 10 μg/ml, monoclonal, mouse, clone 1A4), CD68 (10 μg/ml, monoclonal, mouse, clone 514H12; Abcam, Cambridge, MA), and von Willebrand Factor (vWF, 10 μg/ml, polyclonal, rabbit; Dako, Carpinteria, CA) were detected using immunofluorescent methods. Brightfield and fluorescent images were captured using an Olympus IX51 microscope (Olympus, Tokyo, Japan).

Levels of chromagen indicating positive staining were analyzed semiquantitatively using ImageJ software (NIH) following the protocol outlined by Balaoing et al.[29] First, the background was subtracted from each image using a 150-pixel rolling ball radius. Second, the Color Deconvolution plugin[30] was applied to separate the hematoxylin stain from the chromogenic diaminobenzidine (DAB) channel. Within the DAB channel, the threshold intensity was used to create a binary mask that identified the regions of positive staining after normalization to a negative control tissue sample. The number of pixels that represent staining for an antigen was divided by the total sample area in pixels to generate the percentage of the tissue in the field of view that stained positively for a particular protein.

Microarray Hybridization and Data Analysis

After mechanical homogenization of leaflets, total valvular interstitial cell (VIC) RNA was isolated following the RNeasy (Qiagen, Valencia, CA) fibrous tissue spin-column kit protocol. RNA samples from 3 juvenile and four 2-yo swine were selected for microarray analysis with Affymetrix GeneChip Porcine Genome Arrays (Affymetrix, Santa Clara, CA). Data were processed and analyzed as described previously.[31] Briefly, raw microarray data were background corrected and normalized using the libraries in the Bioconductor Project[32] within the open source statistical language R (v2.15.2; R Foundation for Statistical Computing, Vienna, Austria). A significant genes list was generated after determining differential gene expression between adult and juvenile samples with the Empirical Bayes *t* test statistic.[33]

The processed and annotated data were submitted to Ingenuity iReport (Ingenuity Systems, Redwood City, CA). Using the content in the Ingenuity Knowledge Base, iReport performed an annotation enrichment analysis to map groups of genes to specific biological pathways that were overrepresented in the differentially expressed genes. A *P* value was calculated using the Fisher's exact right-tailed test to assess the probability that the association between each pathway and the genes was not explained by chance alone. These *P* values were adjusted with the Bonferroni correction (0.0500/total number of pathways) to determine significance cutoffs. In compliance with MIAME standards, these data have been deposited in NCBI's Gene Expression Omnibus database (http://www.ncbi.nlm.nih.gov/geo; accession number GSE53997).

Quantitative Reverse-Transcription Polymerase Chain Reaction for Microarray Validation

Quantitative reverse-transcription polymerase chain reaction (qRT-PCR) was employed to validate the gene expression results obtained from microarray analysis on the same 7 samples. The genes selected for validation consisted of a mix of over- and underexpressed genes in the dataset. RNA reverse transcription was carried out using a High Capacity cDNA Reverse Transcription kit (Applied Biosystems, Carlsbad, CA). Taqman Gene Expression Assays (Applied Biosystems) were used for qRT-PCR amplification. Relative expression was determined using the ΔΔCt method,[34] where target genes were first normalized to GAPDH and then relative to RFH juvenile samples. qRT-PCR data were analyzed statistically as outlined below.

Statistical Analysis

Leaflet thickness was measured at 10 different spots across the belly of each leaflet; these values were averaged to obtain the mean thickness per subject. Average thickness per experimental group was acquired by averaging the mean thickness of all subjects within each group. Quantification of chromogen intensity was performed on 3 images per leaflet. The percentage of positive staining was obtained for each image and these percentages were averaged per animal. The mean percentage of positive staining was averaged across the subjects in each experimental group to obtain the mean. Throughout the study, experimental groups were compared to one another with 1-way ANOVA in conjunction with Tukey's honestly significant difference post-test using KaleidaGraph software (Synergy, Reading, PA); *P* values less than or equal to 0.0500 were considered statistically significant. Data are presented as mean±SD.

Results

Adult RFH Swine Develop Complex Atherosclerotic Lesions

Levels of serum cholesterol in RFH swine were significantly higher than those in WT swine (Table 1) and within the range reported for humans with HoFH.[1] Consistent with previous reports,[25] evaluation of the coronary arteries of 2-yo adult RFH swine revealed the presence of advanced atherosclerotic plaques (Figure 1). Invasion of smooth muscle cells, as detected by presence of αSMA, was observed within raised atheromatous regions (Figure 1D); these regions also exhibited evidence of increased lipid oxidation (Figure 1B). Monocyte/macrophage recruitment (indicated by the detection of MCP-1) and presence of lymphocyte degranulation (indicated by visualization of CD107 [LAMP-1]-positive cells; Figure 1C) were also observed. The advanced maturity of the lesions is indicated by the presence of apoptotic cells in areas of or adjacent to plaque formation (Figure 1E).

Extracellular Matrix Remodeling and Thickening Are Evident in Adult RFH Leaflets

Histological examination of aortic valve leaflets from juvenile and adult WT and RFH swine revealed the emergence of numerous hallmarks of early valve disease only in adult RFH animals. A healthy trilaminar structure was observed in juvenile specimens from both WT and RFH animals (Figure 2), where distinct collagen, glycosaminoglycan (GAG), and elastin layers could be identified in the fibrosa, spongiosa, and ventricularis layers, respectively; this is indistinguishable from the arrangement observed in healthy human leaflets.[35] Furthermore, the thickness was uniform throughout the entire length of the juvenile WT and RFH leaflets. When WT animals reached an age of 1 yo, this healthy trilaminar structure and uniform thickness was maintained. In contrast, extensive extracellular matrix (ECM) remodeling and subendothelial thickening were evident in the 1- and 2-yo RFH specimens. Leaflets from adult RFH animals were greatly enriched in proteoglycans, which were deposited between the endothelial layer and elastic lamina and comprised the majority of the thickened area. Disorganized deposition of collagen fibers was also observed in all samples, with fibers appearing in the spongiosa and ventricularis. The elastin in adult RFH leaflets appeared fragmented and was decreased compared to the juvenile leaflets. Von Kossa staining of 2-yo RFH leaflets revealed no evidence of mineralization (not shown). ECM remodeling, as well as the other hallmarks described in this study, were observed in all adult RFH leaflets examined; the images included in the figures are representative of the sample set.

Leaflet sections were measured after histological staining to quantify the extent of thickening observed in adult RFH heart valves. There was no difference in leaflet thickness between juvenile WT and juvenile RFH animals (Table 2). As WT animals aged to 1 yo, leaflet thickness did not change. In contrast, when RFH animals reached 1 yo, leaflet thickness had significantly increased relative to the juveniles. A direct comparison of leaflets from 1-yo WT versus 1-yo RFH swine shows that the average leaflet thickness for RFH swine was more than double that for WT (P=0.0016). This thickening continued to progress with RFH animal age, reaching 1.1 mm at 3 yo. These changes in leaflet microstructure occurred in the absence of changes in valvular interstitial cell proliferation, apoptosis, or αSMA expression (Figures S1 and S2).

ICE Indicates Normal Leaflet Function and Mild Thickening in 3-yo Aortic RFH Valves

As noted above, histological examination clearly indicated significant thickening and ECM reorganization in aortic valve leaflets from adult RFH swine (Figure 2; Table 2), but histological analysis alone is not able to determine whether these changes are sufficient to alter valve function. Thus, ICE was performed to evaluate whether adult RFH swine experienced impaired valve function. In three of the five 3-yo RFH swine, ICE indicated no diagnostic evidence of significant pathology (Figure 3; Video S1). In the remaining two 3-yo RFH animals, there was evidence of mild valvular sclerosis (Figure 3; Video S2), but no evidence of calcification was observed under ultrasound criteria. The limited color Doppler

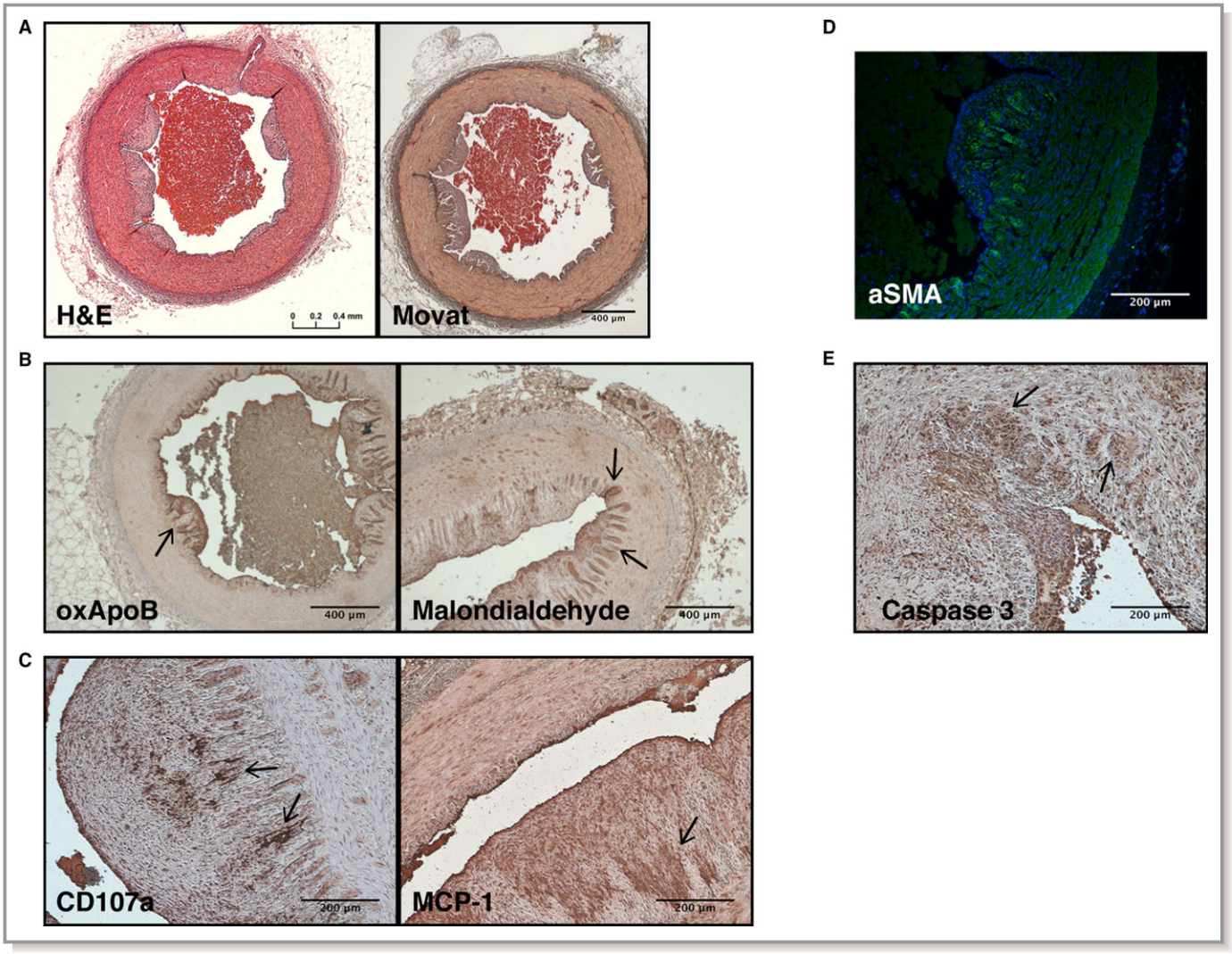

Figure 1. Representative histology of atherosclerotic lesions in the coronary arteries of adult RFH swine. A, Hematoxylin and eosin (H&E) staining and Movat's Pentachrome revealed wall thickening, fibrin accumulation, and plaque buildup in coronary arteries. B, α-SMA-positive cells were detected in the subendothelial region. C, Lipid oxidation was observed by immunostaining of oxApoB and malondialdehyde. D, Apoptotic cells were identified throughout the arteries by immunostaining for caspase 3. E, Leukocyte degranulation (CD107a) and the secretion of MCP-1 were also observed in the intima, as expected in an atherosclerotic plaque. Scale bars: 400 µm (A and C); 200 µm (B, D, and E). Arrows indicate areas representative of positive staining. N=4 animals. MCP-1 indicates monocyte chemoattractant protein-1; oxApoB, oxidatively modified apolipoprotein B; RFH, Rapacz familial hypercholesterolemic; α-SMA, alpha-smooth muscle actin.

examinations from the short axis perspective did not detect any evidence of valvular insufficiency.

Increased Lipid Oxidation Observed in RFH Leaflets

Given that both histological and ICE analyses revealed some early features of CAVD onset in adult RFH swine, we next evaluated WT and RFH leaflets for other features believed to be associated with early-stage valve disease, namely, deposition of oxidized LDL and the presence of inflammation. Leaflet sections were stained for oxApoB, which is the primary apolipoprotein associated with LDL and is mechanistically implicated in the atherosclerotic process,[36] as well as MDA, a product of lipid oxidation and a marker of oxidative stress.[37] In juvenile animals, levels of oxApoB (Figure 4A and 4B) and MDA (Figure 4A and 4C) were similar for both WT and RFH animals. Aging of WT animals to 1 yo did not change expression of either oxApoB or MDA relative to juvenile WT. In contrast, when RFH animals reached 1 yo, there was a significant increase in oxApoB and MDA relative to both the juvenile RFH condition and the 1-yo WT swine. Specifically, ≈20% of the WT and RFH juvenile leaflet area stained positively for oxApoB, and this increased to 80% for 1-yo RFH. In the case of MDA, the increase in staining area went from <20% for WT and juvenile RFH to 44% for 1 yo RFH. MDA

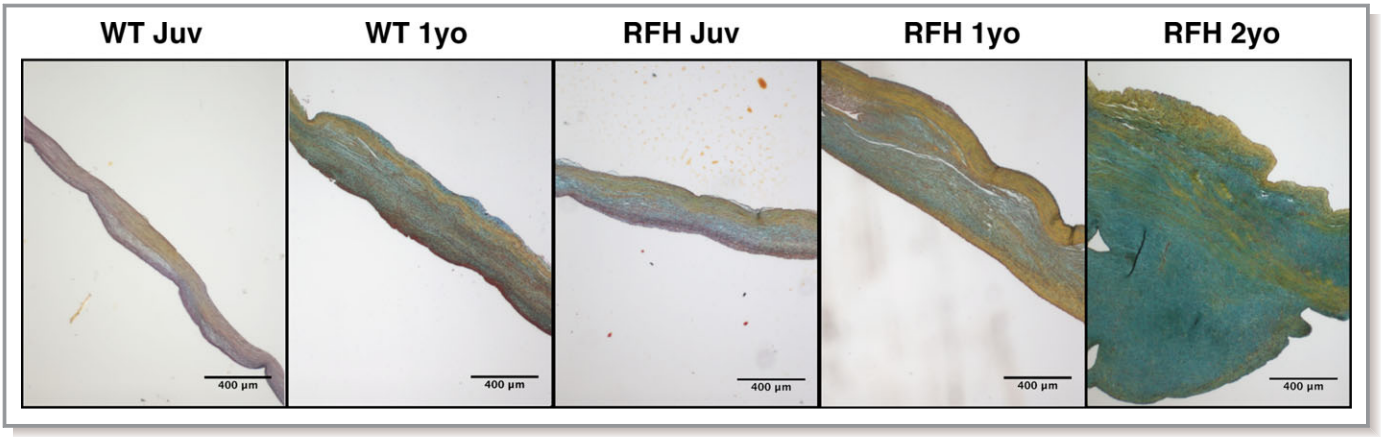

Figure 2. Aortic valve leaflet microarchitecture in juvenile and adult RFH swine. Extensive remodeling of the extracellular matrix in 1- and 2-year-old RFH swine was observed by Movat's Pentachrome staining compared to juvenile RFH swine as well as both juvenile and 1-year-old WT swine. Specifically, adult RFH leaflets exhibited collagen disarray in layers other than the fibrosa, a substantial increase in proteoglycan content, and elastin fragmentation. Thickening of leaflets with age was also evident in RFH swine, whereas the juvenile and 1-year-old WT leaflets remained similar to each other in both architecture and thickness. N=3 to 4 animals/condition, n=3 samples/animal. Scale bar=400 μm. RFH indicates Rapacz familial hypercholesterolemic; WT, wild type.

levels continued to increase with age in RFH swine, reaching 72% of tissue area by 2 yo, and exhibiting strong expression throughout the entire length and thickness of the leaflet. Staining of leaflets from 3-yo RFH swine revealed similar features as those found in 2-yo animals (Figure S3).

Macrophages Infiltrate 2-yo RFH Leaflets

The presence of MCP-1, a chemokine that regulates the infiltration of macrophages, was evaluated in WT and RFH leaflets as an indicator of inflammation (Figure 5A). Leaflets from juvenile WT and RFH swine did not differ in the amount or localization of MCP-1, and these levels remained constant as both WT and RFH swine reached 1 yo (Figure 5B). However, the 2-yo RFH swine exhibited a 6-fold increase in positive MCP-1 staining relative to all other conditions. To verify whether any leukocytes had infiltrated the leaflets, 2-yo RFH samples were stained for CD68, a macrophage marker.

Table 2. Thickness of Leaflets From WT and RFH Swine

Experimental Group	Leaflet Thickness (mm)	*P* Value*
WT Juvenile	0.26 (0.10)	—
WT 1 yo	0.23 (0.04)	0.5486
RFH Juvenile	0.27 (0.12)	0.9871
RFH 1 yo	0.49 (0.03)†	0.0155
RFH 2 yo	0.81 (0.41)†	0.0364
RFH 3 yo	1.1 (0.13)†	0.0015

RFH indicates Rapacz familial hypercholesterolemic; WT, wild-type.
*Compared to WT Juvenile swine.
†Statistically significant; significance cutoff=P<0.0500.

CD68-positive cells were indeed found in 2-yo leaflets, where they localized to thickened areas (Figure 5C).

Microarray Analysis

The gene expression profile of 2-yo RFH VICs was compared to that of juvenile RFH VICs, resulting in the identification of 906 differentially expressed (fold change >2; P<0.0500) transcripts out of 23 256 transcripts present in the

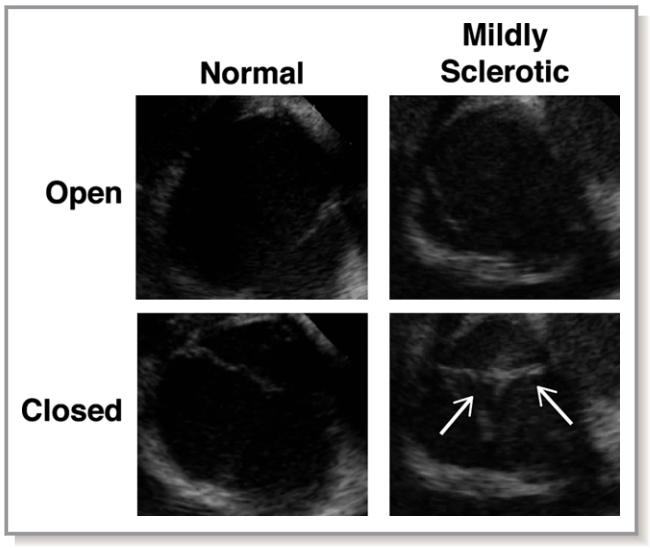

Figure 3. Evaluation of adult RFH aortic valve function. ICE revealed that valve function was not impaired in any of the 3-year-old subjects (left panels). However, mild sclerosis was observed in two 3-year-old swine (right panels, arrows point at thickened leaflets). N=5 animals. ICE indicates intracardiac echocardiography; RFH, Rapacz familial hypercholesterolemic.

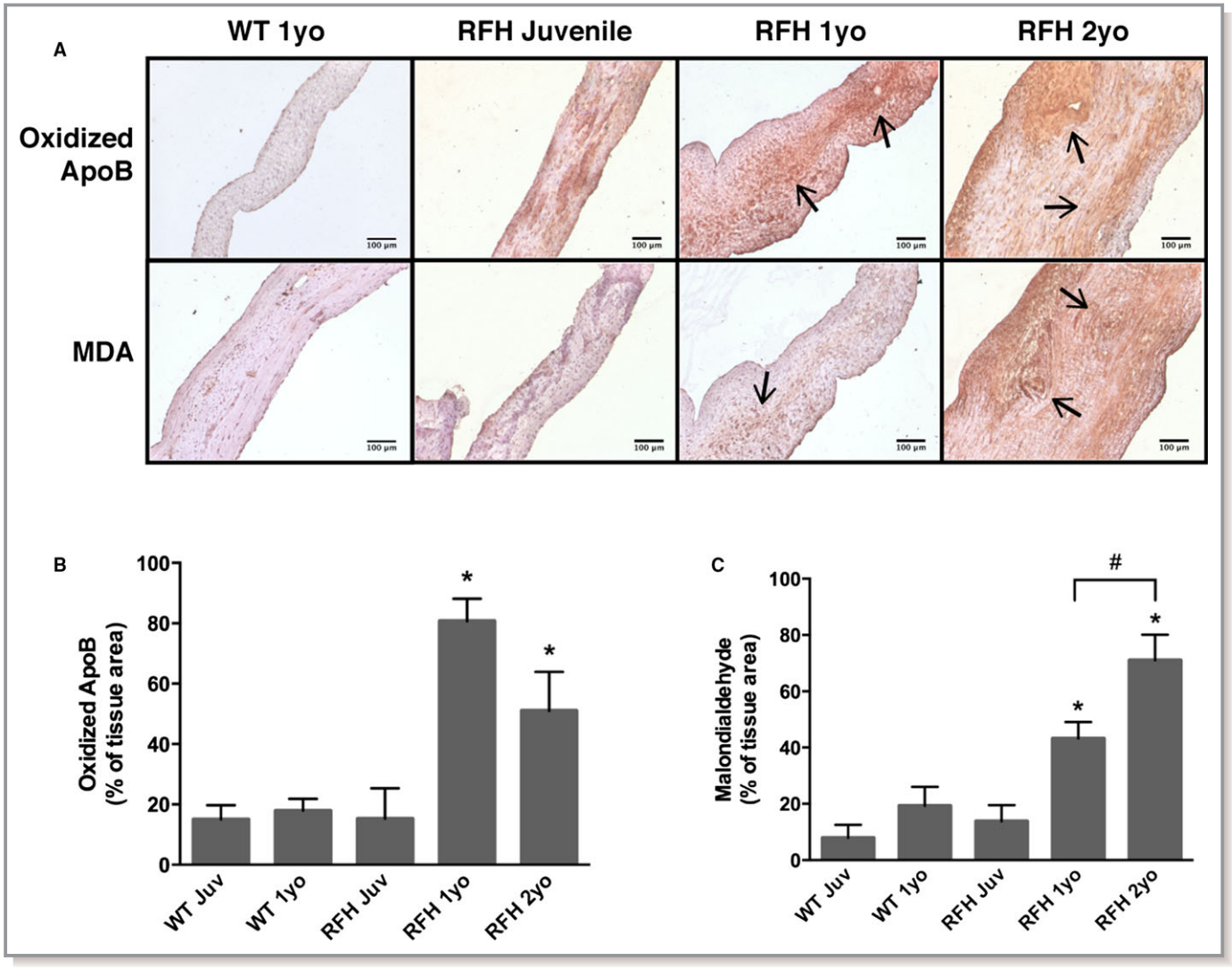

Figure 4. Lipid oxidation in RFH aortic valve leaflets. A, WT and RFH sections were stained for 2 markers of lipid oxidation: oxApoB and MDA. Arrows point to areas representative of positive staining. B, Deposition of oxApoB, the main structural component of low-density lipoprotein, was observed in both WT and RFH leaflets. However, increased oxApoB accumulation of was present in 1- and 2-year-old RFH valves. C, Further evidence of oxidative stress was present in 1- and 2-year-old RFH, but not in WT 1-year-old or RFH juvenile leaflets, as demonstrated by immunostaining for MDA, a product of lipid peroxidation. *P<0.0500 compared to WT 1-year-old swine, $^{\#}P$<0.0500. N=3 to 4 animals/condition, n=3 samples/animal. Scale bars=100 μm. MDA indicates malondialdehyde; oxApoB, oxidatively modified apolipoprotein B; RFH, Rapacz familial hypercholesterolemic; WT, wild type.

GeneChips (Table S1; Figure S4). These 906 transcripts represent 765 genes that map to the Ingenuity Knowledge Base. The top 10 upregulated and top 10 downregulated genes in aortic valves from 2-yo versus juvenile RFH swine are listed in Table 3. Numerous inflammation-related genes (eg, chemokine [C-X-C motif] ligand 14, interleukin [IL]-6, IL-8, and E-selectin) comprised the list of most strongly upregulated genes in adult RFH VICs, whereas several ECM-related genes (eg, elastin, collagen type II, and periostin) were among the most significantly downregulated.

Using the expanded significant genes list, 17 biological pathways were found to be overrepresented in 2-yo RFH VIC samples compared to juvenile samples (Table 4; expanded description in Table S2). Atherosclerosis signaling was identified as one of the over-represented biological pathways. Additionally, of the 17 over-represented biological pathways in valves from 2-yo RFH swine, 5 were also found to be over-represented in a comparison of gene expression profiles between healthy and diseased human aortic valves.[38]

Discussion

Elevated LDL is a strong risk factor for atherosclerosis, and treatments that reduce LDL levels have proven efficacious in reducing CAD[18,19]; this is also true for individuals with FH,

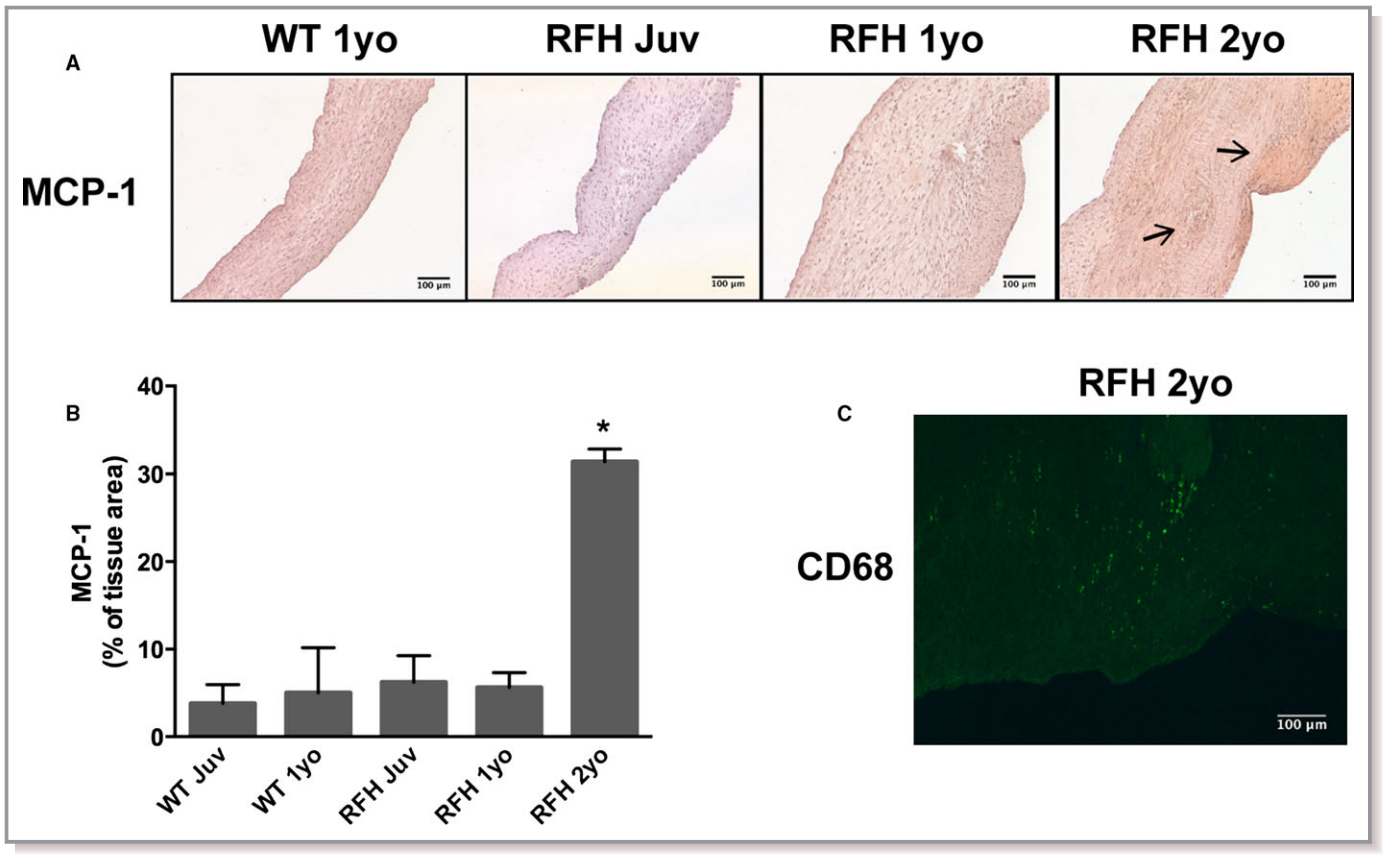

Figure 5. Macrophages infiltrate adult RFH aortic valve leaflets. A, Accumulation of inflammatory marker MCP-1 was observed in 2-year-old RFH swine, but not in 1-year-old WT or RFH swine. B, Presence of MCP-1 in 2-year-old RFH swine was increased ≈3-fold relative to other RFH and WT animals. C, Macrophages were detected only in thickened leaflet areas in 2-year-old RFH swine, as indicated by positive staining for CD68 in areas with thickness >400 μm. N=3 to 4 animals/condition, n=3 samples/animal. Scale bars=100 μm. MCP-1 indicates monocyte chemoattractant protein 1; RFH, Rapacz familial hypercholesterolemic; WT, wild type. **P* < 0.0500 compared to WT 1-year-old swine.

where vascular disease is found in virtually all untreated adult patients with HoFH,[1] and LDL reduction techniques can attenuate or delay its development.[1,17,18] However, the relationship between hypercholesterolemia and CAVD is more ambiguous. Whereas hypercholesterolemia is a risk factor for CAVD, lipid-lowering techniques do not significantly reduce CAVD incidence.[21–23] In both heterozygous FH and HoFH, CAVD prevalence is significantly higher than in the normotypic population, but still occurs at a greatly reduced rate relative to the development of atherosclerosis in FH individuals.[1,8,9,39] By examining the aortic valves from an FH animal model known to recapitulate the atherosclerotic events of human HoFH with high fidelity, we sought to better understand the relationship between hypercholesterolemia and development of CAVD. Because RFH swine have a uniform gene mutation, are fed identical diets, are free from other comorbidities, and can be sacrificed in exact age-matched cohorts, they provide a highly controlled system in which to study this relationship. A secondary goal of the work was evaluation of whether RFH swine may serve as an appropriate animal model for development of human-like CAVD.

The findings from this study demonstrate that, though adult RFH swine formed complex atherosclerotic lesions and a more advanced valvular disease state than has been previously achieved with swine[40] (ie, significant thickening, extensive ECM remodeling, lipid oxidation, and inflammation), they did not develop advanced aortic stenosis or calcified valve lesions. This absence of valvular calcification or stenosis in RFH swine was unlikely to be a result of insufficient animal age. RFH swine develop atherosclerosis on a similar developmental time frame as humans with HoFH (ie, by mid-late adolescence for both of these groups[41,42]); meanwhile, the adult age of the RFH swine studied herein is well past the porcine equivalent of the average age of CAVD diagnosis in humans with HoFH (17.9 years).[41] Limited histological examination of elderly RFH pigs (Figure S5) also did not show any progression of valvular pathology beyond what was present by 2 to 3 yo. Together, these results suggest that atherosclerosis and CAVD may share an initial disease process that then diverges, with additional comorbidities necessary for progression of CAVD past early-stage events.

Table 3. Top 10 Genes Up- and Downregulated in 2 yo Versus Juvenile RFH Leaflets

Gene Symbol	Gene Name	Fold Change
Upregulated		
CXCL14	Chemokine (C-X-C motif) ligand 14	128.0
IL6	Interleukin-6 (interferon, beta 2)	78.8
NR4A3	Nuclear receptor subfamily 4, group A, member 3	29.9
HSPA6	Heat shock 70 kDa protein 6	24.3
DUSP5	Dual specificity phosphatase 5	21.1
IL8	Interleukin 8	16.0
FOXJ3	FBJ murine osteosarcoma viral oncogene homolog B	14.9
FOSB	Forkhead box J3	14.9
FABP4	Fatty acid-binding protein 4, adipocyte	13.9
SELE	Selectin E	12.1
Downregulated		
HBD	Hemoglobin, delta	−16.0
HBA1/HBA2	Hemoglobin, alpha 1	−14.9
ADAMTS17	ADAM metallopeptidase thrombospondin type 1 motif, 17	−12.1
POSTN	Periostin, osteoblast specific factor	−8.6
DYNC1I2	Dynein, cytoplasmic 1, intermediate chain 2	−8.0
TNC	Tenascin C	−7.5
ETV6	Transcription factor ets variant 6	−7.0
IFI44L	Interferon-induced protein 44-like	−7.0
COL2A1	Collagen, type II, alpha 1	−7.0
ELN	Elastin	−6.5

Statistical analysis of the microarray data identified 906 differentially expressed transcripts mapping to 765 differentially expressed genes (see Table S1 for an expanded list). RFH indicates Rapacz familial hypercholesterolemic.

Table 4. Significant Biological Pathways in a Microarray Study Comparing 2 yo and Juvenile RFH Valvular Interstitial Cells

Pathways	DEGs*	*P* Value†
Role of macrophages, fibroblasts and endothelial cells in rheumatoid arthritis	30	7.80E-06
Role of osteoblasts, osteoclasts and chondrocytes in rheumatoid arthritis	29	2.19E-08
Glucocorticoid receptor signaling	25	6.78E-05
Atherosclerosis signaling	24	9.48E-11
Dendritic cell maturation	24	2.54E-07
Granulocyte adhesion and diapedesis	22	2.17E-06
IL-6 signaling‡	20	4.25E-08
Hepatic fibrosis/hepatic stellate cell activation‡	20	8.90E-07
Acute phase response signaling‡	20	1.84E-05
Agranulocyte Adhesion and Diapedesis	20	6.30E-05
Aryl Hydrocarbon Receptor Signaling	18	1.54E-05
LXR/RXR activation‡	17	8.06E-06
IL-10 signaling‡	15	7.16E-08
TREM1 signaling	13	5.41E-07
Communication between innate and adaptive immune cells	13	7.74E-05
PPAR signaling	13	1.09E-04
IL-17A signaling in fibroblasts	9	7.94E-06

Compared to chance alone, the pathways presented in this list contain an over-representation of differentially expressed genes (up- and down-regulated). Most of the pathways in this list are related to inflammation and the immune system. DEGs indicates differentially expressed, mapped genes; RFH, Rapacz familial hypercholesterolemic.
*The number of genes that were found to meet the *P*-value and fold change cutoffs AND map to a gene in the Ingenuity Knowledge Base.
†Adjusted significance cutoff=$P<0.0030$.
‡Moreover, some pathways were also found to be significant in a microarray dataset by Bossé et al comparing healthy and diseased human aortic valve leaflets.

Insights Into Early CAVD Provided by Adult RFH Swine

Characterization of events in early CAVD in humans has been challenging owing to the scarcity of valve specimens that become available at this stage of disease. However, the ability to study early stages of CAVD is valuable because even mild-to-moderate CAVD is known to increase all-cause and cardiovascular mortality.[43,44] The RFH swine examined in the current work appear to offer a model that recapitulates numerous critical features of early CAVD and may thus be useful for studying the initiation and early progression of this disease. Though juvenile WT and RFH animals were identical in all measured outcomes, significant differences between these groups emerged by 1 year of age. Leaflets from 1-yo RFH swine exhibited a doubling in thickness, significant ECM rearrangement, and deposition of oxidized lipids relative to their juvenile counterpart. Meanwhile, the leaflets from 1-yo WT animals were identical to those from juvenile WT swine, indicating that the observed changes in 1-yo RFH leaflets were not simply a product of normal aging.

Both histological evaluation and echocardiography revealed thickening of leaflets from adult RFH swine. Although thickening alone is not a predictor of CAVD, it is considered one of the earliest events in the pathological process.[45] The normal trilayered structure of the valve ECM was disrupted in adult RFH leaflets, indicating that the thickening was not merely a consequence of aging, but was instead pathological in nature. The thickened areas were found between the endothelial layer and elastic lamina and were rich in proteoglycans, which is consistent with the

histology of human valves in the earliest stages of CAVD,[46,47] as well as the recent description of valves from adolescent swine fed a hypercholesterolemic diet.[40] Other pathological ECM changes found in humans, such as collagen fiber disorganization and elastin fragmentation,[35,46,48] were also evident in all adult RFH specimens. Interestingly, the list of the 10 most downregulated genes in adult RFH swine was populated with several ECM proteins, such as elastin, periostin, tenascin C, and collagen type II, which may also be an indicator of ECM dysregulation. Although their exact contribution to the progression of CAVD remains to be elucidated, these structural features are particularly noteworthy because the ECM is thought to play an important role in the regulation of leaflet mechanics and valve cell biology.[49]

Lipid oxidation has been associated with CAVD and is postulated to be one of the key pathological mechanisms that lead to altered cell and valvular biology.[50,51] oxApoB, the primary lipoprotein present in LDL, was abundant in adult RFH valves and coronary arteries as early as 1 yo. It is possible that its accumulation is related to the matrix disarray also observed in adult RFH leaflets; increased levels of oxLDL have been found to correlate with increased valve remodeling in human aortic stenosis.[52] Likewise, MDA, the most prevalent aldehyde product of lipid peroxidation (LPO), was also expressed abundantly and exclusively in adult RFH leaflets. Although the precise role of MDA and other reactive aldehydes in valvular disease is unknown, their level increases in blood plasma from atherosclerotic patients, and the lesions themselves have been shown to contain varying degrees of LPO-specific aldehydes.[37] Furthermore, accumulation of oxApoB preceded that of MDA in adult RFH valves, suggesting that oxLDL underwent further oxidation processes while entrapped in the leaflet ECM. The prevalence of oxidized lipids in RFH leaflets also supports the conclusion that these valves are undergoing early CAVD processes, rather than myxomatous degeneration, a condition that is also characterized by GAG enrichment and collagen disruption. In addition to aortic valve myxomatous degeneration being rare in humans who do not also have congenital abnormalities or inflammation-related disease,[53] non-rheumatic myxomatous human aortic valves tend to not be highly enriched in oxidized lipids,[54] nor is hypercholesterolemia believed to be a risk factor for myxomatous aortic valve disease.

Hyperlipidemia is frequently accompanied by inflammation in both human and animal diseased valves,[50,55,56] and this was also the case in RFH swine, where macrophages infiltrated thickened areas of adult leaflets. Our results indicate that leaflet thickening and lipid oxidation preceded the emergence of inflammation. Although this finding is consistent with the ability of oxLDL to regulate macrophage activation and stimulate macrophage recruitment,[45,55] the current study is the first to clearly show the sequence of this CAVD hallmark progression, which has important implications for understanding the process and potential treatment of CAVD. Microarray analysis of adult versus juvenile RFH VICs also strongly implicated the upregulation of inflammatory processes in adult RFH pigs, with numerous inflammation-related genes populating the list of significantly upregulated genes.

Finally, the list of over-represented biological pathways that emerged as a result of the microarray analysis of juvenile versus adult RFH swine possessed substantial overlap with the list of biological pathways identified in a microarray study of diseased versus healthy human valves.[38] Five of the 8 over-represented pathways in the human data set[38] were also over-represented in the current RFH study, specifically: IL-6 signaling, hepatic fibrosis/hepatic stellate cell activation, acute-phase response signaling, liver X receptor/retinoid X receptor activation, and IL-10 signaling. These findings further suggest that RFH swine are able to recapitulate features of human CAVD. The microarray results also supported the conclusion that the observed valve pathology was likely early CAVD, rather than myxomatous degeneration, given that mouse studies have shown that increased chondrogenic gene expression accompanies myxomatous aortic valve disease,[57,58] but the RFH swine exhibited significantly downregulated expression of numerous chondrogenic genes (eg, *COL2A1*, *ASPN*, *HAPLN*, and *COL4A1*).

Relationship Between CAVD and Atherosclerosis

As an established model of atherosclerosis that is generated by a naturally occurring gene mutation, RFH swine may also help elucidate the relationship between atherosclerosis and CAVD. The evidence surrounding the relationship between these diseases has been seemingly contradictory, given that they exhibit similar disease characteristics and have significant overlap of risk factors, yet only a small fraction of humans with atherosclerosis develop CAVD.[59] Several investigators have postulated that atherosclerosis and CAVD share a common disease process with chronic inflammation at its core,[60] but that progression of CAVD past the early-stage atherosclerotic-like valve lesion requires additional cofactors, such as other genetic markers or metabolic conditions.[59] Our histological analysis of coronary arteries and aortic valves from adult RFH swine yielded results that are consistent with the hypothesis of a shared initial disease process that is linked to inflammation, with further stimulation or comorbidities necessary to induce more-advanced CAVD. These observations are further supported by our microarray data, which yielded a list of significantly upregulated genes that was

primarily populated with inflammation-related factors, and which showed atherosclerosis signaling as an over-represented pathway in the adult RFH swine data set. A similar microarray study comparing the vascular wall of healthy and atherosclerotic RFH peripheral arteries also identified an upregulation of inflammation-related genes in the diseased phenotype.[61]

Comparison to Other Animal Models of CAVD

Although performed in the context of FH and aortic valve disease, the application of insights gained from the characterization of valves from RFH swine does not need to be limited to the study of only FH-related disease. The search for an animal model of CAVD that accurately mimics human anatomy and physiology and recapitulates key CAVD hallmarks is an ongoing effort motivated by the need to better understand the etiology and progression of CAVD in FH and non-FH individuals alike. Though mice and rabbits are commonly used for this purpose, these animals exhibit numerous dissimilarities from humans with respect to valve properties and lipid metabolism, as reviewed elsewhere.[56] Despite their numerous cardiovascular and genetic similarities with humans, swine have been underexplored as CAVD models, perhaps because the large size of standard swine can make such de novo development of an animal model an unwieldy and risky endeavor. A recent study of full-sized Yorkshire swine fed a high-fat, high-cholesterol diet found that these swine also developed only early-stage indicators of CAVD, such as ECM disarray.[40] This may have been attributable to the young age of the swine (<6 months old), or this animal model may be intrinsically limited to experiencing only mild valvular disease. Meanwhile, the RFH swine used in the current study were equivalent to middle-aged adults, meaning that animal age is unlikely to be the reason for the absence of more-advanced valvular disease in this work, given that the CAVD diagnosis in humans with HoFH is typically made by the teenage years.[41] Thus, our analysis of RFH swine is supportive of the hypothesis that additional stimulation beyond hypercholesterolemia is needed to develop advanced CAVD, which is also likely the case with humans. RFH swine do also possess several advantages over other swine models, such as their relatively small size (weight at 6 months is 31 kg for RFH versus 100 kg for Yorkshire) and the genetic basis of their hypercholesterolemia, rendering them highly relevant to the human FH population, as well as potentially facilitating the future addition of comorbidities. Additionally, RFH swine are capable of recapitulating the process of arterial restenosis, whereas the conventional Yorkshire swine do not,[27] further emphasizing their utility in modeling human cardiovascular pathophysiology.

Study Limitations

One of the unique and powerful aspects of this study was the use of pigs of relatively advanced age. Due to the costs and logistical difficulties associated with the care of these large animals, it is rare for any research study to use swine past the age of 6 months. The advanced age of the RFH swine was an important element in the current study, given that it decreased the likelihood that the absence of CAVD was a consequence of insufficient animal age; this has been a significant limitation in many other studies. Unfortunately, one limitation introduced by the use of aged swine is a somewhat reduced sample size. However, as demonstrated by our results, there was a low degree of variability across animals within each age group, and the sample sizes used herein were sufficient to produce statistical significance across multiple outcomes. An additional obstacle introduced by using aged swine is that their overall size and large thorax present significant challenges in performing quantitative echocardiographic measurements of their aortic valves. This is a known challenge, even in smaller pigs, owing to porcine chest anatomy and heart alignment,[62,63] but the problem becomes particularly acute in swine >100 kg.

Another potential limitation of this study was the use of exclusively female animals because of behavioral challenges in maintaining herds of adult male pigs. In humans, male sex is associated with a 2-fold increase in the risk of aortic valve disease.[13] Moreover, recent work has shown sex-related differences at the cellular level between male and female VICs isolated from fresh porcine leaflets,[64] wherein male VICs appeared to be predisposed to assuming a diseased phenotype when compared to female VICs. Thus, it is possible that the mild degree of CAVD achieved in our RFH swine was also influenced by the sex of the animals, and that more extensive CAVD may be accomplished by using male animals. Finally, the WT background for RFH swine was only recently developed, and this study used the most aged animals available from this herd. None of the previous publications describing the use of RFH swine as models for atherosclerosis and restenosis have included a background-matched WT control.[24–27]

Conclusions

Based upon in vivo imaging, histological assessment, and gene expression profiling, our findings indicate that RFH swine develop valvular pathology that reproduces numerous critical features characteristic of early-stage human CAVD. Meanwhile, these animals exhibited advanced atherosclerosis, indicating that FH alone is sufficient for progression of vascular, but not valvular, stenosis. Together, these results suggest that

atherosclerosis and CAVD may share an initial disease process that then diverges, with additional comorbidities necessary for progression of CAVD past early-stage events. Additionally, with its intrinsic hypercholesterolemia, the RFH pig may represent a useful tool for investigating the effects of combined disease processes (eg, diabetes and metabolic syndrome) on the development of CAVD to address the question of how CAVD progresses beyond the initial atherosclerotic-like lesion.

Sources of Funding

This work was supported by the National Heart, Lung, and Blood Institute and the National Institute of Biomedical Imaging and Bioengineering at the National Institutes of Health (R01-HL093281 and R21-EB019508; to Masters), as well as a predoctoral fellowship from the American Heart Association (15PRE 22170006; to Porras).

Disclosures

None.

References

1. Cuchel M, Bruckert E, Ginsberg HN, Raal FJ, Santos RD, Hegele RA, Kuivenhoven JA, Nordestgaard BG, Descamps OS, Steinhagen-Thiessen E, Tybjaerg-Hansen A, Watts GF, Averna M, Boileau C, Boren J, Catapano AL, Defesche JC, Hovingh GK, Humphries SE, Kovanen PT, Masana L, Pajukanta P, Parhofer KG, Ray KK, Stalenhoef AF, Stroes E, Taskinen MR, Wiegman A, Wiklund O, Chapman MJ. Homozygous familial hypercholesterolaemia: new insights and guidance for clinicians to improve detection and clinical management. A position paper from the Consensus Panel on Familial Hypercholesterolaemia of the European Atherosclerosis Society. *Eur Heart J*. 2014;35:2146–2157.
2. Civeira F; International Panel on Management of Familial H. Guidelines for the diagnosis and management of heterozygous familial hypercholesterolemia. *Atherosclerosis*. 2004;173:55–68.
3. Varghese MJ. Familial hypercholesterolemia: a review. *Ann Pediatr Cardiol*. 2014;7:107–117.
4. Nordestgaard BG, Chapman MJ, Humphries SE, Ginsberg HN, Masana L, Descamps OS, Wiklund O, Hegele RA, Raal FJ, Defesche JC, Wiegman A, Santos RD, Watts GF, Parhofer KG, Hovingh GK, Kovanen PT, Boileau C, Averna M, Boren J, Bruckert E, Catapano AL, Kuivenhoven JA, Pajukanta P, Ray K, Stalenhoef AF, Stroes E, Taskinen MR, Tybjaerg-Hansen A; European Atherosclerosis Society Consensus P. Familial hypercholesterolaemia is underdiagnosed and undertreated in the general population: guidance for clinicians to prevent coronary heart disease: consensus statement of the European Atherosclerosis Society. *Eur Heart J*. 2013;34:3478–3490a.
5. Goldstein JL, Brown MS. Regulation of low-density lipoprotein receptors: implications for pathogenesis and therapy of hypercholesterolemia and atherosclerosis. *Circulation*. 1987;76:504–507.
6. Raal FJ, Santos RD. Homozygous familial hypercholesterolemia: current perspectives on diagnosis and treatment. *Atherosclerosis*. 2012;223:262–268.
7. Marks D, Thorogood M, Neil HA, Humphries SE. A review on the diagnosis, natural history, and treatment of familial hypercholesterolaemia. *Atherosclerosis*. 2003;168:1–14.
8. Kawaguchi A, Miyatake K, Yutani C, Beppu S, Tsushima M, Yamamura T, Yamamoto A. Characteristic cardiovascular manifestation in homozygous and heterozygous familial hypercholesterolemia. *Am Heart J*. 1999;137:410–418.
9. Rajamannan NM, Edwards WD, Spelsberg TC. Hypercholesterolemic aortic-valve disease. *N Engl J Med*. 2003;349:717–718.
10. Rajamannan NM, Evans FJ, Aikawa E, Grande-Allen KJ, Demer LL, Heistad DD, Simmons CA, Masters KS, Mathieu P, O'Brien KD, Schoen FJ, Towler DA, Yoganathan AP, Otto CM. Calcific aortic valve disease: not simply a degenerative process: a review and agenda for research from the National Heart and Lung and Blood Institute Aortic Stenosis Working Group. Executive summary: calcific aortic valve disease-2011 update. *Circulation*. 2011;124:1783–1791.
11. O'Brien KD, Reichenbach DD, Marcovina SM, Kuusisto J, Alpers CE, Otto CM. Apolipoproteins B, (a), and E accumulate in the morphologically early lesion of 'degenerative' valvular aortic stenosis. *Arterioscler Thromb Vasc Biol*. 1996;16:523–532.
12. Olsson M, Thyberg J, Nilsson J. Presence of oxidized low density lipoprotein in nonrheumatic stenotic aortic valves. *Arterioscler Thromb Vasc Biol*. 1999;19:1218–1222.
13. Stewart BF, Siscovick D, Lind BK, Gardin JM, Gottdiener JS, Smith VE, Kitzman DW, Otto CM. Clinical factors associated with calcific aortic valve disease. Cardiovascular Health Study. *J Am Coll Cardiol*. 1997;29:630–634.
14. Loomba RS, Arora R. Statin therapy and aortic stenosis: a systematic review of the effects of statin therapy on aortic stenosis. *Am J Ther*. 2010;17:e110–e114.
15. Cowell SJ, Newby DE, Prescott RJ, Bloomfield P, Reid J, Northridge DB, Boon NA. A randomized trial of intensive lipid-lowering therapy in calcific aortic stenosis. *N Engl J Med*. 2005;352:2389–2397.
16. Liebe V, Brueckmann M, Borggrefe M, Kaden JJ. Statin therapy of calcific aortic stenosis: hype or hope? *Eur Heart J*. 2006;27:773–778.
17. Rodenburg J, Vissers MN, Wiegman A, van Trotsenburg AP, van der Graaf A, de Groot E, Wijburg FA, Kastelein JJ, Hutten BA. Statin treatment in children with familial hypercholesterolemia the younger, the better. *Circulation*. 2007;116:664–668.
18. Smilde TJ, van Wissen S, Wollersheim H, Trip MD, Kastelein JJ, Stalenhoef AF. Effect of aggressive versus conventional lipid lowering on atherosclerosis progression in familial hypercholesterolaemia (ASAP): a prospective, randomised, double-blind trial. *Lancet*. 2001;357:577–581.
19. Steinberg D. Thematic review series: the pathogenesis of atherosclerosis. An interpretive history of the cholesterol controversy, part V: the discovery of the statins and the end of the controversy. *J Lipid Res*. 2006;47:1339–1351.
20. Kang S, Wu Y, Li X. Effects of statin therapy on the progression of carotid atherosclerosis: a systematic review and meta-analysis. *Atherosclerosis*. 2004;177:433–442.
21. Nishimura RA, Otto CM, Bonow RO, Carabello BA, Erwin JP III, Guyton RA, O'Gara PT, Ruiz CE, Skubas NJ, Sorajja P, Sundt TM III, Thomas JD, Anderson JL, Halperin JL, Albert NM, Bozkurt B, Brindis RG, Creager MA, Curtis LH, DeMets D, Hochman JS, Kovacs RJ, Ohman EM, Pressler SJ, Sellke FW, Shen WK, Stevenson WG, Yancy CW. 2014 AHA/ACC guideline for the management of patients with valvular heart disease: a report of the American College of Cardiology/American Heart Association Task Force on Practice Guidelines. *J Thorac Cardiovasc Surg*. 2014;148:e1–e132.
22. Rossebo AB, Pedersen TR, Boman K, Brudi P, Chambers JB, Egstrup K, Gerdts E, Gohlke-Barwolf C, Holme I, Kesaniemi YA, Malbecq W, Nienaber CA, Ray S, Skjaerpe T, Wachtell K, Willenheimer R. Intensive lipid lowering with simvastatin and ezetimibe in aortic stenosis. *N Engl J Med*. 2008;359:1343–1356.
23. Chan KL, Teo K, Dumesnil JG, Ni A, Tam J. Effect of lipid lowering with rosuvastatin on progression of aortic stenosis: results of the aortic stenosis progression observation: measuring effects of rosuvastatin (ASTRONOMER) trial. *Circulation*. 2010;121:306–314.
24. Hasler-Rapacz J, Ellegren H, Fridolfsson AK, Kirkpatrick B, Kirk S, Andersson L, Rapacz J. Identification of a mutation in the low density lipoprotein receptor gene associated with recessive familial hypercholesterolemia in swine. *Am J Med Genet*. 1998;76:379–386.
25. Getz GS, Reardon CA. Animal models of atherosclerosis. *Arterioscler Thromb Vasc Biol*. 2012;32:1104–1115.
26. Schinkel AF, Krueger CG, Tellez A, Granada JF, Reed JD, Hall A, Zang W, Owens C, Kaluza GL, Staub D, Coll B, Ten Cate FJ, Feinstein SB. Contrast-enhanced ultrasound for imaging vasa vasorum: comparison with histopathology in a swine model of atherosclerosis. *Eur J Echocardiogr*. 2010;11:659–664.
27. Tellez A, Krueger CG, Seifert P, Winsor-Hines D, Piedrahita C, Cheng Y, Milewski K, Aboodi MS, Yi G, McGregor JC, Crenshaw T, Reed JD, Huibregtse B, Kaluza GL, Granada JF. Coronary bare metal stent implantation in homozygous LDL receptor deficient swine induces a neointimal formation pattern similar to humans. *Atherosclerosis*. 2010;213:518–524.
28. Swinkels DW, Demacker PN. Comparative studies on the low density lipoprotein subfractions from pig and man. *Comp Biochem Physiol B*. 1988;90:297–300.
29. Balaoing LR, Post AD, Liu H, Minn KT, Grande-Allen KJ. Age-related changes in aortic valve hemostatic protein regulation. *Arterioscler Thromb Vasc Biol*. 2014;34:72–80.

30. Ruifrok AC, Johnston DA. Quantification of histochemical staining by color deconvolution. *Anal Quant Cytol Histol*. 2001;23:291–299.
31. Porras AM, Shanmuganayagam D, Meudt JJ, Krueger CG, Reed JD, Masters KS. Gene expression profiling of valvular interstitial cells in Rapacz familial hypercholesterolemic swine. *Genom Data*. 2014;2:261–263.
32. Gentleman RC, Carey VJ, Bates DM, Bolstad B, Dettling M, Dudoit S, Ellis B, Gautier L, Ge Y, Gentry J, Hornik K, Hothorn T, Huber W, Iacus S, Irizarry R, Leisch F, Li C, Maechler M, Rossini AJ, Sawitzki G, Smith C, Smyth G, Tierney L, Yang JY, Zhang J. Bioconductor: open software development for computational biology and bioinformatics. *Genome Biol*. 2004;5:R80.
33. Smyth GK. Linear models and empirical bayes methods for assessing differential expression in microarray experiments. *Stat Appl Genet Mol Biol*. 2004;3:Article3.
34. Livak KJ, Schmittgen TD. Analysis of relative gene expression data using real-time quantitative PCR and the 2(-Delta Delta C(T)) method. *Methods*. 2001;25:402–408.
35. Latif N, Sarathchandra P, Taylor PM, Antoniw J, Yacoub MH. Localization and pattern of expression of extracellular matrix components in human heart valves. *J Heart Valve Dis*. 2005;14:218–227.
36. Imes CC, Austin MA. Low-density lipoprotein cholesterol, apolipoprotein B, and risk of coronary heart disease: from familial hyperlipidemia to genomics. *Biol Res Nurs*. 2013;15:292–308.
37. Uchida K. Role of reactive aldehyde in cardiovascular diseases. *Free Radic Biol Med*. 2000;28:1685–1696.
38. Bosse Y, Miqdad A, Fournier D, Pepin A, Pibarot P, Mathieu P. Refining molecular pathways leading to calcific aortic valve stenosis by studying gene expression profile of normal and calcified stenotic human aortic valves. *Circ Cardiovasc Genet*. 2009;2:489–498.
39. Rallidis L, Naoumova RP, Thompson GR, Nihoyannopoulos P. Extent and severity of atherosclerotic involvement of the aortic valve and root in familial hypercholesterolaemia. *Heart*. 1998;80:583–590.
40. Sider KL, Zhu C, Kwong AV, Mirzaei Z, de Lange CF, Simmons CA. Evaluation of a porcine model of early aortic valve sclerosis. *Cardiovasc Pathol*. 2014;23:289–297.
41. Kolansky DM, Cuchel M, Clark BJ, Paridon S, McCrindle BW, Wiegers SE, Araujo L, Vohra Y, Defesche JC, Wilson JM, Rader DJ. Longitudinal evaluation and assessment of cardiovascular disease in patients with homozygous familial hypercholesterolemia. *Am J Cardiol*. 2008;102:1438–1443.
42. Hamamdzic D, Wilensky RL. Porcine models of accelerated coronary atherosclerosis: role of diabetes mellitus and hypercholesterolemia. *J Diabetes Res*. 2013;2013:761415.
43. Rosenhek R, Klaar U, Schemper M, Scholten C, Heger M, Gabriel H, Binder T, Maurer G, Baumgartner H. Mild and moderate aortic stenosis. Natural history and risk stratification by echocardiography. *Eur Heart J*. 2004;25:199–205.
44. Volzke H, Haring R, Lorbeer R, Wallaschofski H, Reffelmann T, Empen K, Rettig R, John U, Felix SB, Dorr M. Heart valve sclerosis predicts all-cause and cardiovascular mortality. *Atherosclerosis*. 2010;209:606–610.
45. Cosmi JE, Kort S, Tunick PA, Rosenzweig BP, Freedberg RS, Katz ES, Applebaum RM, Kronzon I. The risk of the development of aortic stenosis in patients with "benign" aortic valve thickening. *Arch Intern Med*. 2002;162:2345–2347.
46. Otto CM, Kuusisto J, Reichenbach DD, Gown AM, O'Brien KD. Characterization of the early lesion of 'degenerative' valvular aortic stenosis. Histological and immunohistochemical studies. *Circulation*. 1994;90:844–853.
47. Kuusisto J, Rasanen K, Sarkioja T, Alarakkola E, Kosma VM. Atherosclerosis-like lesions of the aortic valve are common in adults of all ages: a necropsy study. *Heart*. 2005;91:576–582.
48. Hinton RB Jr, Lincoln J, Deutsch GH, Osinska H, Manning PB, Benson DW, Yutzey KE. Extracellular matrix remodeling and organization in developing and diseased aortic valves. *Circ Res*. 2006;98:1431–1438.
49. Chen JH, Simmons CA. Cell-matrix interactions in the pathobiology of calcific aortic valve disease: critical roles for matricellular, matricrine, and matrix mechanics cues. *Circ Res*. 2011;108:1510–1524.
50. Rossebo AB, Pedersen TR. Hyperlipidaemia and aortic valve disease. *Curr Opin Lipidol*. 2004;15:447–451.
51. Rajamannan NM. Low-density lipoprotein and aortic stenosis. *Heart*. 2008;94:1111–1112.
52. Cote C, Pibarot P, Despres JP, Mohty D, Cartier A, Arsenault BJ, Couture C, Mathieu P. Association between circulating oxidised low-density lipoprotein and fibrocalcific remodelling of the aortic valve in aortic stenosis. *Heart*. 2008;94:1175–1180.
53. Waller BF, Howard J, Fess S. Pathology of aortic valve stenosis and pure aortic regurgitation: a clinical morphologic assessment—Part II. *Clin Cardiol*. 1994;17:150–156.
54. Lars W, Thora S, Mats B. Role of inflammation in nonrheumatic, regurgitant heart valve disease. A comparative, descriptive study regarding apolipoproteins and inflammatory cells in nonrheumatic heart valve disease. *Cardiovasc Pathol*. 2007;16:171–178.
55. Steinberg D. Atherogenesis in perspective: hypercholesterolemia and inflammation as partners in crime. *Nat Med*. 2002;8:1211–1217.
56. Sider KL, Blaser MC, Simmons CA. Animal models of calcific aortic valve disease. *Int J Inflam*. 2011;2011:364310.
57. Cheek JD, Wirrig EE, Alfieri CM, James JF, Yutzey KE. Differential activation of valvulogenic, chondrogenic, and osteogenic pathways in mouse models of myxomatous and calcific aortic valve disease. *J Mol Cell Cardiol*. 2012;52:689–700.
58. Fang M, Alfieri CM, Hulin A, Conway SJ, Yutzey KE. Loss of beta-catenin promotes chondrogenic differentiation of aortic valve interstitial cells. *Arterioscler Thromb Vasc Biol*. 2014;34:2601–2608.
59. Mazzone A, Venneri L, Berti S. Aortic valve stenosis and coronary artery disease: pathophysiological and clinical links. *J Cardiovasc Med (Hagerstown)*. 2007;8:983–989.
60. Freeman RV, Otto CM. Spectrum of calcific aortic valve disease: pathogenesis, disease progression, and treatment strategies. *Circulation*. 2005;111:3316–3326.
61. Bahls M, Bidwell CA, Hu J, Tellez A, Kaluza GL, Granada JF, Krueger CG, Reed JD, Laughlin MH, Van Alstine WG, Newcomer SC. Gene expression differences during the heterogeneous progression of peripheral atherosclerosis in familial hypercholesterolemic swine. *BMC Genom*. 2013;14:443.
62. Crick SJ, Sheppard MN, Ho SY, Gebstein L, Anderson RH. Anatomy of the pig heart: comparisons with normal human cardiac structure. *J Anat*. 1998;193:105–119.
63. Kerut EK, Valina CM, Luka T, Pinkernell K, Delafontaine P, Alt EU. Technique and imaging for transthoracic echocardiography of the laboratory pig. *Echocardiography*. 2004;21:439–442.
64. McCoy CM, Nicholas DQ, Masters KS. Sex-related differences in gene expression by porcine aortic valvular interstitial cells. *PLoS One*. 2012;7:e39980.